AUTONOMOUS MATHEMATICAL OPTIMIZATION OF CONTINUOUS CASTING PROCESSES

Wilfried Schäfer, Götz Hartmann, Erik Hepp, MAGMA GmbH, Aachen, Germany
Dieter G. Senk, Sonja Stratemeier, IEHK RWTH Aachen University, Germany

ABSTRACT

Over many years, the liquid metal flow in steel continuous casting tundishes and moulds, the cooling and solidification of the melt and the formation of segregation, as well as stresses and cracks have been the subject of numerous projects in which the phenomena were analyzed by various measurement techniques, calculations and/or analytical or numerical simulations. The motivation for these efforts was the desire to understand the details of the phenomena influencing the casting process performance and the strand quality, in order to be able to optimize the casting process conditions.

Today, the combination of newest developments in coupled 3D numerical heat and mass transport simulation coupled with computational optimization methods based on genetic algorithms allows new approaches to answering various questions that arise in continuous casting process optimization.

This contribution introduces a numerical simulation based optimization strategy, following rigorous thermodynamic and thermo mechanical models as well as a strictly methodic approach.

KEYWORDS

Mathematical Optimization, Process Simulation, Heat Transfer, Liquid Pool Depth, Reverse Engineering, Spray Cooling, Genetic Algorithm, MOGA

INTRODUCTION

Simulation technologies need the input of start and boundary conditions, usually given by engineers. Considering theses conditions, models are applied to all kinds of mechanical, physical or chemical processes, and simulation tells the engineer what results he might expect when going through a process as defined by him.

It is a trial and error driven, iterative process, that requires an engineer’s interpretation and decision after any of the simulation runs. It is an old dream of the engineers, to leave most of the required decision supporting and decision finding processes to a computer, thus being unburdened and able to concentrate on decisions which can not be made by computers. This contribution presents a computational optimization methodology, based on numerical simulations of the continuous casting process as the first step into the future of autonomous process optimization - recently being named as “the second generation of numerical simulation technologies” /1/.

In order to get the best possible boundary conditions for a continuous casting process simulation, it is proposed to first determine characteristic process conditions such as heat transfer coefficients between strand and mould. An inverse optimization method has been used to minimize the differences between measured and simulated mould temperature/time plots, where the simulated plots were generated through variation of the relevant heat transfer coefficients. The appropriate heat transfer coefficients for further simulations were those that lead to the best fit of measured and simulated temperature/time plots.

These process conditions were then used as boundary conditions for the autonomous numerical casting process optimization. The objectives for the optimization were to get the best possible coupling between casting speed, spraying nozzle layout and liquid pool depth.

The use of a multi-objective optimization algorithm made it possible to follow all these objectives simultaneously. The Pareto-set from the optimization allows the evaluation of how the different versions that were simulated perform with respect to the given objectives – which means selecting a situation that makes the best possible compromise.

1. MEASURED MOULD AND BILLET TEMPERATURES

Early studies on heat transfer and skin formation in a continuous casting mould on bench scale were done by Singh and Blazek /2/. The temperatures in the copper mould as well as surface temperatures 25 mm below the mould were measured. A study on mould flux lubrication was carried out by Pinheiro et al. /3/, where mould temperatures were monitored for different mould powder compositions. The influence of steel grade, powder composition and cooling water velocity has been estimated. The instrumentation of the mould with thermocouples is in some degree well documented. Industrial trials conducted at four companies to study mould heat transfer were reported by Chandra et al. /4/. At Hoogovens the influence of different parameter, e.g. steel grade, on heat flux profiles was studied /5/. Terauchi et al. estimated heat flux in the meniscus region by thermocouple measurements in a mould of a pilot continuous casting machine /6/. Even though it is common practice to measure temperature gradients in the mould there is a lack in well documented plant data for billet casting. For the purpose of developing and validating simulation models for the continuous casting process it is necessary to compare simulation results with recorded temperature curves from copper moulds. In this paper the “measured” temperature/time plots are taken from a simulation study where such plots were generated. This approach was necessary due to the above mentioned lack in well documented plant data.

3. HEAT WITHDRAWAL IN THE MOULD

The transported heat from the strand surface to the cooling water is conducted through the solidified steel shell, the flux layer, the gas gap, the copper wall before convective dissipated to the cooling water. For a steady state heat transfer the heat flow is given by:

$$\dot{Q} = \alpha_{eff} \cdot (\vartheta_u - \vartheta_0) \cdot A$$

where α_{eff} is the effective heat transfer coefficient. The reciprocal $1/\alpha_{eff}$ is the heat transmission resistance consisting of the resistances of the different layers between strand surface and copper wall. The heat flux through a layer of casting flux is complicated due to the complex structures of the flux layer, the glassy and crystalline state, respectively, the mushy and liquid part as well as microscopically gas gaps. In order to simplify the details of the radiation and convection heat transfer through a slag layer with several sub layers an engineering approach is considered, where the conduction and radiation properties of the slag layer, and the contact resistance are concentrated in an average “system conductivity” λ_{sys} /7/. To measure the system conductivity in laboratory scale, experimental setups where developed and the dependence of slag composition was investigated /8/. Among the composition, the system conductivity depends on temperature.

4. USE OF GENETIC ALGORITHMS

An effective engine for this automatic optimization is MOGA, the multi object genetic algorithm. This algorithm has two features, being of particular importance in the context of process simulation: It supports the tracking of several independent targets and can handle any type of process and design variables including those variables occurring in continuous casting simulation.
The application of genetic algorithms requires the definition of a start generation consisting of several individuals. In this context "individual" is just another word for design resp. a variant of the involved project. The individuals can be selected resp. generated by using different DOE strategies like random, quasi-random (Sobol), full/reduced factorial, Taguchi or Monte Carlo methods /9/.
The algorithm now starts for any of these individuals a casting process simulation and evaluates the results for their compliance with the given constraints and optimization targets. After that the algorithm creates a new generation following the genetic rules of heredity, mutation and selection. Out of the total number of designs (a given number of generations multiplied by a given number of individuals), being defined and evaluated by the algorithm, we usually get several good designs.
In common it makes no sense to talk about "the optimum" or "the best solution" of a problem, because in almost any optimization task related to casting process simulation we get a set of good designs especially for multi-objective problems. The aim of the design optimization is to find a good compromise out of many possibilities; it is not to calculate an extreme of a function in the mathematical sense.

The optimization described in this paper was performed using the software module MAGMAfrontier.

In this module the user describes the problem by determining some parameters:

- design variables with their corresponding ranges of variation (these are the parameters of the simulation that will be varied)
- output variables (they contain the results of the simulation in concentrated form)
- constraints
- objectives (maximize or minimize certain combinations of output variables)

After all the information is available an optimization loop can be started.

5. DETAILED PROJECT DESCRIPTION

As an example the production of a bloom with a square section of 160 x 160 mm was analysed. The thermo physical properties of a steel grade St52 for the simulation were taken from the database of MAGMASOFT. Six cooling zones with different heat transfer coefficients in each zone were modelled. As casting velocity 3 m/min was chosen. Results of the influence of casting velocities to the depth of the liquid pool were already shown in earlier publications /10/. For the first part of the project the focus was on the heat withdrawal in the mould. With the help of measured temperatures in the mould a heat transfer coefficient should be determined using genetic algorithms.

5.1 REVERSE ENGINEERING OF HEAT TRANSFER COEFICCIENT

Boundary conditions are needed for the computer-aided simulation. Heat transfers, however, that arises while cooling a copper plate in a contiuous casting mould cannot be measured directly.

The best possible, if not the only way to get heat transfer coefficients between mould and strand is to retrieve them from a comparison between measured temperature plots at the same positions to calculated temperature plots. Using a computational optimization method the heat transfers are modified to minimize the difference between measured and calculated temperature plots. Such a problem is called an inverse problem. In this case not the casting proecess is optimized, but a dataset of the simulation.

For the simulation a three dimensional model of the mould and the complete strand has to be set up. The position of "virtual thermocouples" in the geometric model has to correspond exactly with the thermocouple position of the instrumented mould. Fig 1. shows schematic some of the defined control points.

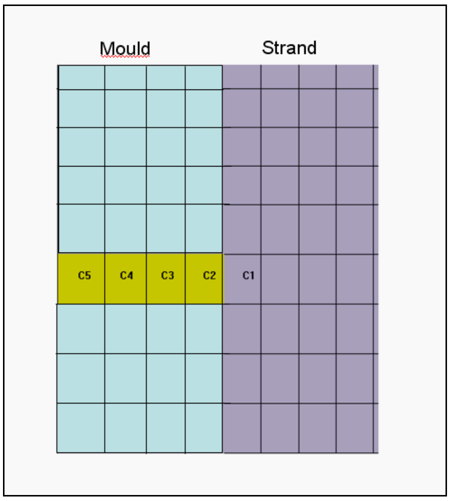

Fig. 1: Definition of control points as virtual thermocouples in the simulation mesh

The idea was to have at different heights in the mould one control point in the strand near to the surface and four control points in uniform distances in the mould. For the optimization the next step is then to define an objective function. In the described example the deviation between measured and simulated temperatures should be minimized by variations of heat transfer coefficients between mould and strand. Therefore the measured curves have to be selected. This is shown in Fig. 2.

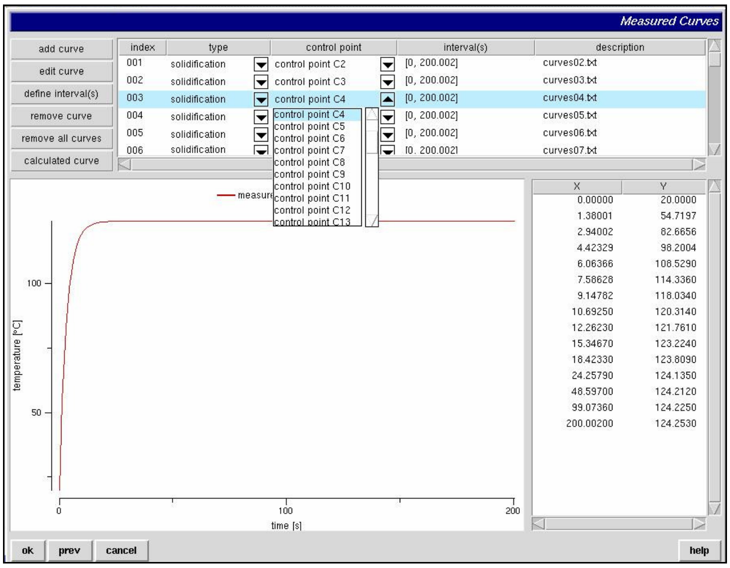

index	type	control point	interval(s)	description
001	solidification	control point C2	[0, 200.002]	curves02.txt
002	solidification	control point C3	[0, 200.002]	curves03.txt
003	solidification	control point C4	[0, 200.002]	curves04.txt
004	solidification	control point C4 control point C5 control point C6 control point C7 control point C8 control point C9 control point C10 control point C11 control point C12 control point C13	[0, 200.002]	curves05.txt
005	solidification		[0, 200.002]	curves06.txt
006	solidification		[0, 200.002]	curves07.txt

X	Y
0.00000	20.0000
1.38001	54.7197
2.94002	82.6656
4.42329	98.2004
6.06366	108.5290
7.58628	114.3360
9.14782	118.0340
10.69250	120.3140
12.26230	121.7610
15.34670	123.2240
18.42330	123.8090
24.25790	124.1350
48.59700	124.2120
99.07360	124.2250
200.00200	124.2530

Fig. 2: Selection of measured temperatures curves as input for the optimization

The heat transfer coefficients between mould and strand and its characteristics can be described by just a few parameters. These parameters are varied by the optimization algorithms until a minimum of the deviation between measured and calculated temperature/time plots is stated. The set of heat transfer coefficients that leads to the minimum is then the parameter set what leads - same meaning, just different words – to the best fit between simulation and measurements.

In the here described project the melt level in the mould is at ca. 150 mm. So the starting point at 6000 W/m^{2}K is only an approximation, but in general such a curve should have a shape as shown in Fig. 3.

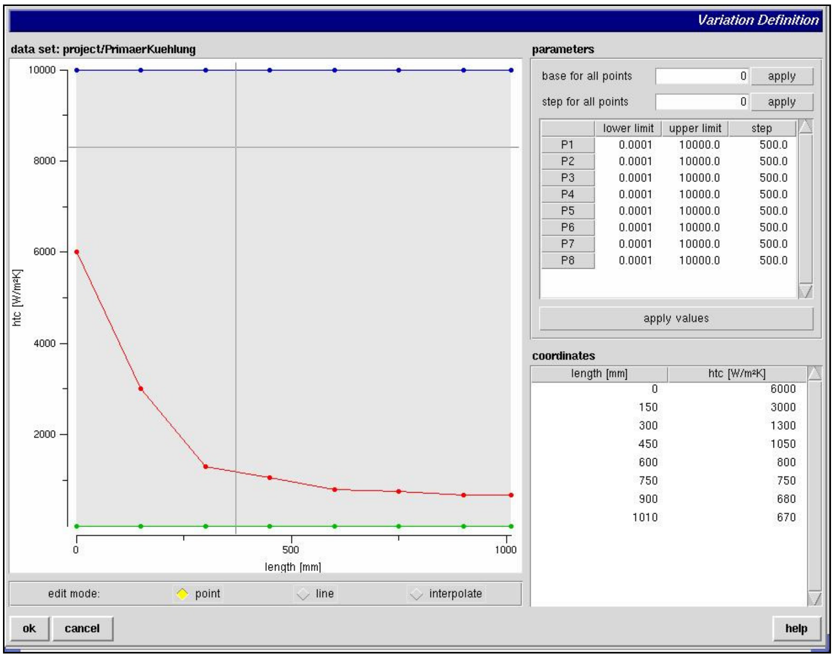

base for all points 0

step for all points 0

	lower limit	upper limit	step
P1	0.0001	10000.0	500.0
P2	0.0001	10000.0	500.0
P3	0.0001	10000.0	500.0
P4	0.0001	10000.0	500.0
P5	0.0001	10000.0	500.0
P6	0.0001	10000.0	500.0
P7	0.0001	10000.0	500.0
P8	0.0001	10000.0	500.0

length [mm]	htc [W/m²K]
0	6000
150	3000
300	1300
450	1050
600	800
750	750
900	680
1010	670

edit mode: ● point ○ line ○ interpolate

Fig. 3: Typical plot of heat transfers between a water cooled copper mould and a strand. This characteristic curve plot can be described by a small number of parameters.

It was expected that the deviation between measurement and simulation would be quite big for the first simulated variants of the heat transfer coefficients (Fig. 4).

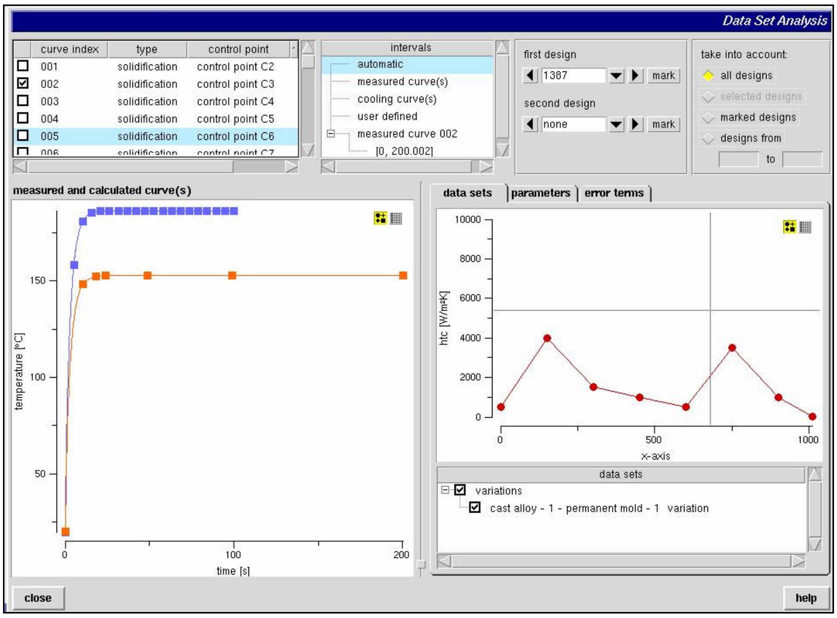

	curve index	type	control point
☐	001	solidification	control point C2
☑	002	solidification	control point C3
☐	003	solidification	control point C4
☐	004	solidification	control point C5
☐	005	solidification	control point C6

Fig. 4: Comparison of measured (orange) and calculated (blue) temperature plots at the beginning of the optimization. On the right the corresponding heat transfer coefficient is visualized.

To get information about the progress of the optimization simulation it is possible to look at the deviation from the mean per each simulated generation (Fig. 5).

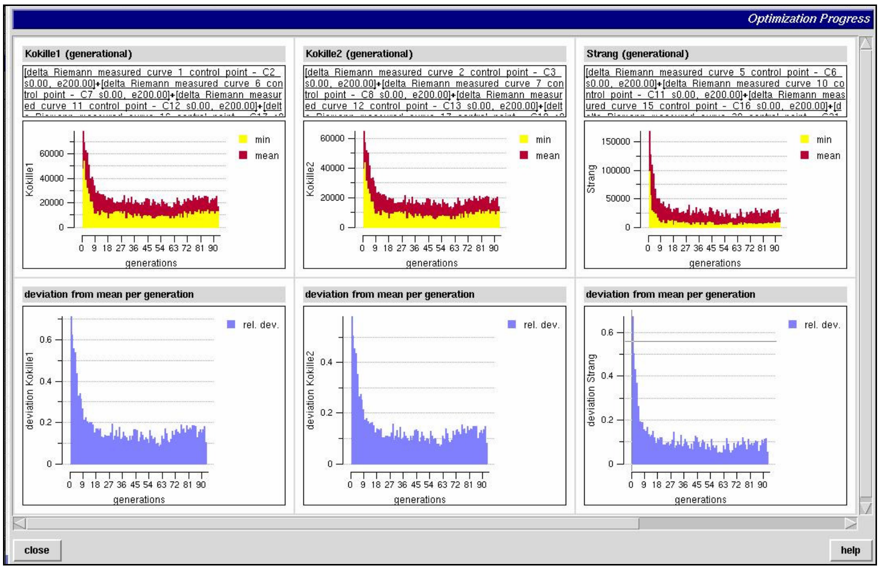

[delta Riemann measured curve 1 control point - C2 s0.00, e200.00]+[delta Riemann measured curve 6 control point - C7 s0.00, e200.00]+[delta Riemann measured curve 11 control point - C12 s0.00, e200.00]+[delt

[delta Riemann measured curve 2 control point - C3 s0.00, e200.00]+[delta Riemann measured curve 7 control point - C8 s0.00, e200.00]+[delta Riemann measured curve 12 control point - C13 s0.00, e200.00]+[delt

[delta Riemann measured curve 5 control point - C6 s0.00, e200.00]+[delta Riemann measured curve 10 control point - C11 s0.00, e200.00]+[delta Riemann measured curve 15 control point - C16 s0.00, e200.00]+[d

Fig. 5: The above plots show clearly, that after some first generations the minimization of the deviation is good enough and the problem converges.

After the optimization the measured and the calculated temperature plots show a good matching (Fig. 6) and the heat transfer coefficient have been identified well.

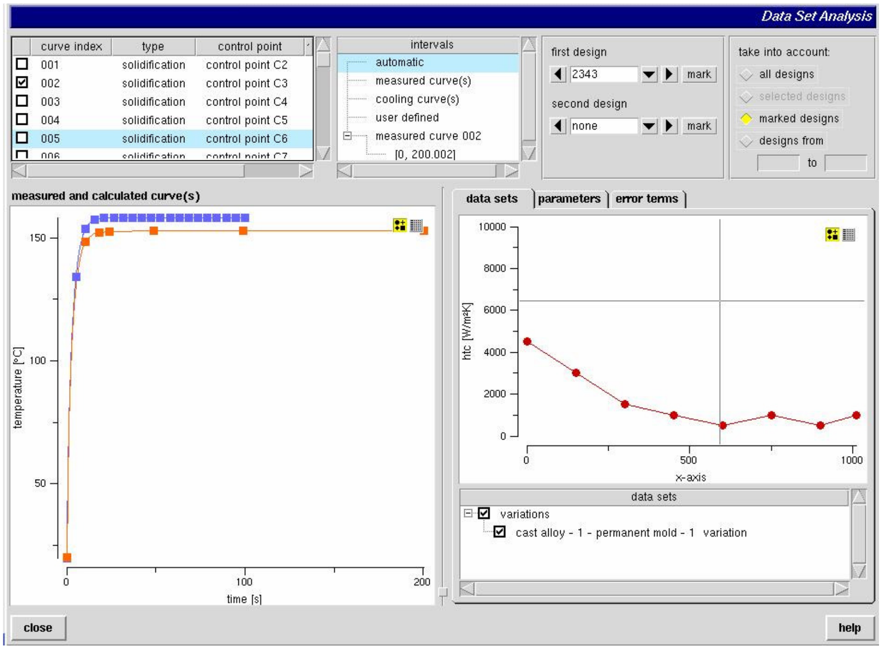

	curve index	type	control point
☐	001	solidification	control point C2
☑	002	solidification	control point C3
☐	003	solidification	control point C4
☐	004	solidification	control point C5
☐	005	solidification	control point C6
☐	006	solidification	control point C7

☑ variations
☑ cast alloy - 1 - permanent mold - 1 variation

Fig. 6: The two temperature curves are now in a good agreement. The corresponding heat transfer coefficient is show on the right.

The variant with the heat transfer coefficient from Figure 6 shows the following distribution of the strand temperature in the mould (Fig. 7).

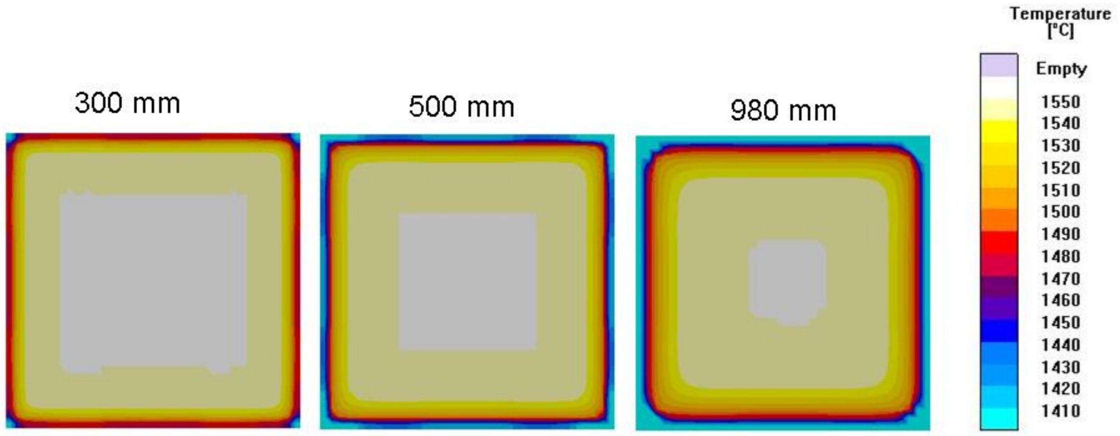

Fig. 7: Temperature distribution of the strand’s cross section at three different heights within the mould, 300mm, 500mm and 980mm from the top edge of the mould with a total length of 1000 mm.

The corresponding surface temperatures of the mould are visualised in Fig. 8. The surface temperatures of the mould decreases as expected after the solidified shell is formed.

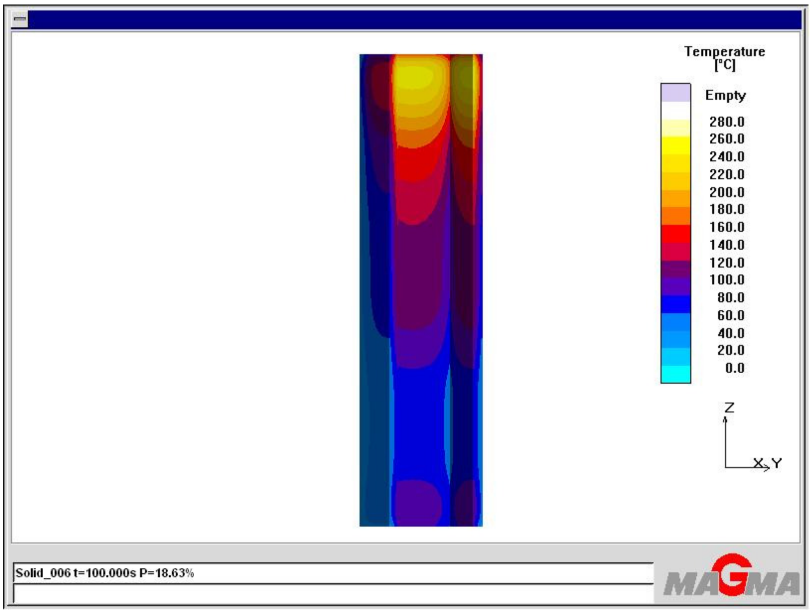

Solid_006 t=100.000s P=18.63%

Fig. 8: Temperature distribution in the mould. Shown is the version where the optimized heat transfer coefficient was used.

5.2 USE OF THE DETERMINED HTC's IN PROCESS OPTIMIZATION

The results of the inverse optimization were used in the second step for the optimization of spraying conditions with the objective of a stable liquid pool depth. Now the optimization is not used to solve an inverse problem, it is used for the optimization of process parameters. The objective function for this part of the project was defined by minimizing the difference between a liquid pool depth resulting from particular secondary cooling parameters and the desired liquid pool depth of 16.5 meters. The variants were the characteristics of the secondary cooling zones (Fig. 9).

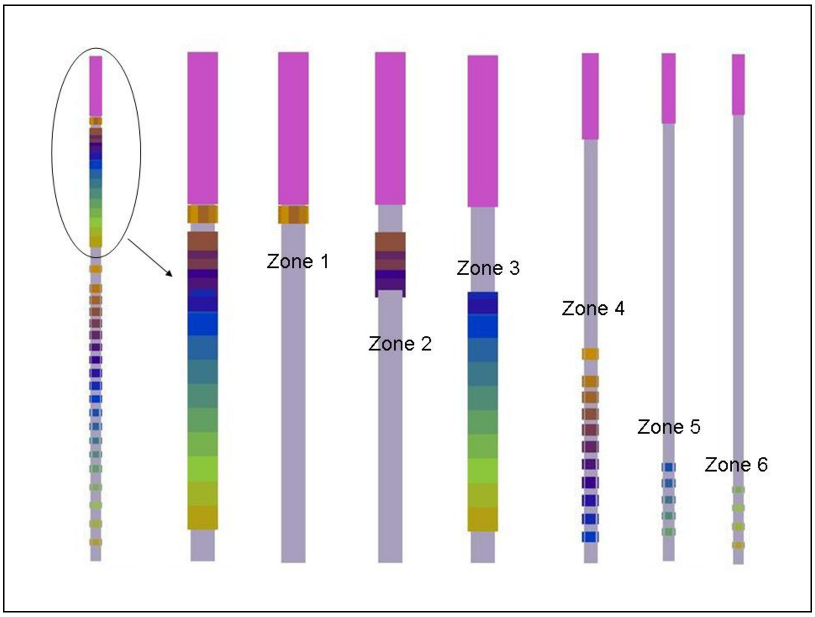

Fig. 9: The secondary cooling is partitioned into 6 different zones; the left picture shows the cooling zones in total.

For the optimization a DOE was generated for various heat transfer coefficients of the secondary cooling in the different zones. As soon as the simulation converged a first look was taken to the sensitivity analysis. This typical result from an optimization run show very clear which cooling zone shows more effect by changing the heat transfer coefficient and which cooling zones are more or less without influence. Zone 3 has the most influence and Zone 6 is nearly without influence and could therefore be neglected (Fig. 10).

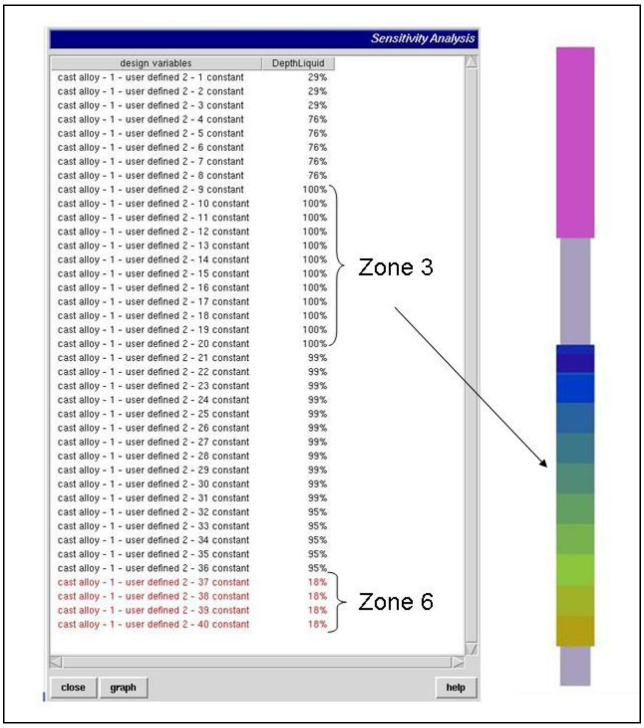

design variables	DepthLiquid
cast alloy - 1 - user defined 2 - 1 constant	29%
cast alloy - 1 - user defined 2 - 2 constant	29%
cast alloy - 1 - user defined 2 - 3 constant	29%
cast alloy - 1 - user defined 2 - 4 constant	76%
cast alloy - 1 - user defined 2 - 5 constant	76%
cast alloy - 1 - user defined 2 - 6 constant	76%
cast alloy - 1 - user defined 2 - 7 constant	76%
cast alloy - 1 - user defined 2 - 8 constant	76%
cast alloy - 1 - user defined 2 - 9 constant	100%
cast alloy - 1 - user defined 2 - 10 constant	100%
cast alloy - 1 - user defined 2 - 11 constant	100%
cast alloy - 1 - user defined 2 - 12 constant	100%
cast alloy - 1 - user defined 2 - 13 constant	100%
cast alloy - 1 - user defined 2 - 14 constant	100%
cast alloy - 1 - user defined 2 - 15 constant	100%
cast alloy - 1 - user defined 2 - 16 constant	100%
cast alloy - 1 - user defined 2 - 17 constant	100%
cast alloy - 1 - user defined 2 - 18 constant	100%
cast alloy - 1 - user defined 2 - 19 constant	100%
cast alloy - 1 - user defined 2 - 20 constant	100%
cast alloy - 1 - user defined 2 - 21 constant	99%
cast alloy - 1 - user defined 2 - 22 constant	99%
cast alloy - 1 - user defined 2 - 23 constant	99%
cast alloy - 1 - user defined 2 - 24 constant	99%
cast alloy - 1 - user defined 2 - 25 constant	99%
cast alloy - 1 - user defined 2 - 26 constant	99%
cast alloy - 1 - user defined 2 - 27 constant	99%
cast alloy - 1 - user defined 2 - 28 constant	99%
cast alloy - 1 - user defined 2 - 29 constant	99%
cast alloy - 1 - user defined 2 - 30 constant	99%
cast alloy - 1 - user defined 2 - 31 constant	99%
cast alloy - 1 - user defined 2 - 32 constant	95%
cast alloy - 1 - user defined 2 - 33 constant	95%
cast alloy - 1 - user defined 2 - 34 constant	95%
cast alloy - 1 - user defined 2 - 35 constant	95%
cast alloy - 1 - user defined 2 - 36 constant	95%
cast alloy - 1 - user defined 2 - 37 constant	18%
cast alloy - 1 - user defined 2 - 38 constant	18%
cast alloy - 1 - user defined 2 - 39 constant	18%
cast alloy - 1 - user defined 2 - 40 constant	18%

Fig. 10: A sensitivity analysis shows the relative contribution of changing heat transfer coefficients to the objective to realize the desired liquid pool depth. The biggest contribution comes from Zone 3.

An important medium to study the results of an optimization project are the so called scatter charts. Here the position of the liquid pool tip is plotted over the water spray nozzle 2-37 in zone 6 (Fig. 11). On the x-coordinate the heat transfer coefficient of a spray nozzle is plotted and the y-coordinate shows the liquid pool depth. For one constant value of heat transfer coefficient for the chosen spray nozzle the y-coordinate shows the variation of heat transfer coefficients for the other zones. The scatter charts shows no tendency, which does mean that there is more or less no influence of changing e.g. the amount of water or the pressure in this zone to the position of the liquid pool tip. This result is in accordance to the sensitivity analysis as shown in Fig. 10.

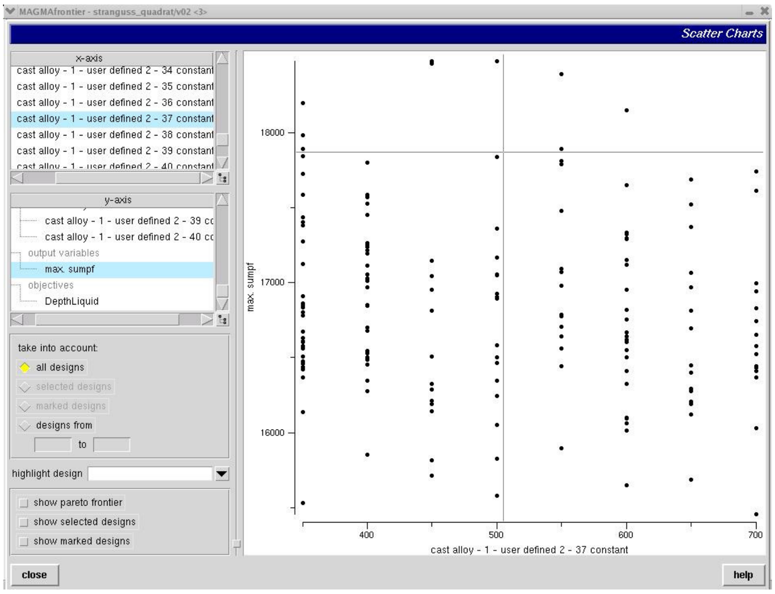

Fig. 11: Scatter chart for the water spray nozzle 2-37 which belongs to the zone 6; no tendency can be found.

Other then the nozzles in zone 6 with almost no influence a spraying nozzle from zone 3 shows significant influence as shown in the sensitivity analysis, see scatter chart (Fig. 12). Now a clear tendency can be found. Changing the heat transfer coefficient to higher amounts will decrease the depth of the liquid pool.

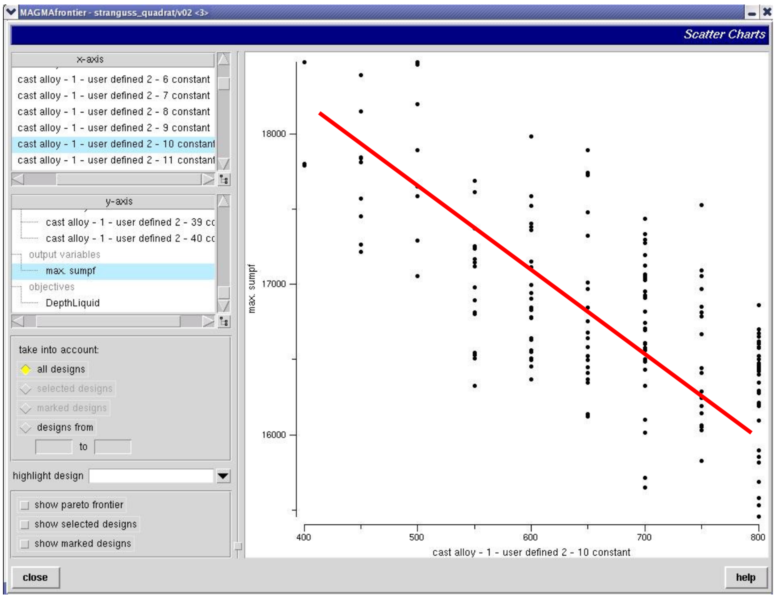

Fig. 12: Scatter chart for the water spray nozzle 2-10 which belongs to the zone 3; a clear tendency can be found.

After this optimization loop the user has now the possibility to choose a design which is corresponding to the desired liquid pool depth. For this design the results can than be studied in detail. Fig. 13 shows as example the result of the calculated liquid pool depth (LPD). This is in the example of course 16.5 meters.

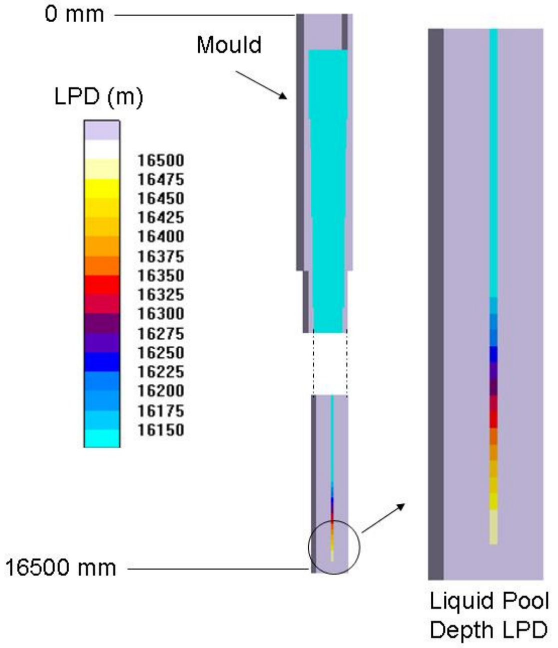

Fig. 13: Result of the calculated liquid pool depth with heat transfer coefficients from the optimization.

6. CONCLUSIONS

It was shown with two examples that autonomous mathematical optimization can be used for the continuous casting process. Based on measured temperatures from several locations in the mould the heat transfer coefficients between strand and mould were calculated with inverse calculations. The heat transfer coefficient is the alternative value for the system conductivity.

The second optimization was done to determine the heat transfer coefficients at secondary cooling nozzles that are suitable to get a stable liquid pool depth at the desired position. From the necessary heat transfer coefficients the water flow rate and pressure can be determined. It was also shown that the individual zones have different influence on the liquid pool depth.

Other optimization objectives can be easily defined to optimize the continuous casting process, taken into account e.g. thermal stresses.

REFERENCES

1.) I. HAHN, G. HARTMANN "Selbständige Rechnerische Optimierung von Druckgussteilen und –Prozessen", Konstruktion, Springer / VDI Verlag, March 2008.
2.) S.N. SINGH, K.E.BLAZEK, Journal of Metals 26, (1974), p.17
3.) C.A.M. PINHEIRO, I.V. SAMARASEKERA, J.K. BRIMACOMBE, B.N. WALKER, Ironmaking & Steelmaking 27, (2000), p. 37
4.) S. CHANDRA, I.V. SAMARASEKERA, J.K. BRIMACOMBE, I.A. BAKSHI, B.N. WALKER, Ironmaking and Steelmaking 23, (1996), p. 512
5.) J.L. LAGERBERG, D.W. VAN DER PLAS, 2th. Europ. Conf. On Continuous Casting, Düsseldorf (1994), METEC Congress, p. 162

6.) M. TERAUCHI, H. NAKATA, ECCC, European Conference on Continuous Casting, 5, Nice, France, 2005
7.) K. SCHWERDTFEGER, The Making, Shaping and Treating of Steel, 11th. Ed., Casting Volume, the AISE Foundation, (2003), Chapter 4, p.1
8.) J.-F. HOLZHAUSER, K.-H. SPITZER, K. SCHWERDTFEGER, Steel Research 70, (1999), p. 252
9.) V: KOKOT, P: BERNBECK "Integration and Application of Optimization Algorithms with Castin Process Simulation", Proceedings from MCWASP 2003, Destin, TMS
10.) E. HEPP, P. BERNBECK, W. SCHÄFER, D. SENK, S. STRATEMEIER "New Developments for Process Modelling of the Continuous Casting of Steel", SteelSim 2007, Graz/Seggau, Austria, p. 203